

p-Wave Superconductivity near a transverse saturation field

K. Hattori and H. Tsunetsugu

*Institute for Solid State Physics, University of Tokyo,
Kashiwanoha 5-1-5, Kashiwa, Chiba 277-8581, Japan*

(Dated: May 6, 2018)

We investigate reentrant superconductivity in an Ising ferromagnetic superconductor URhGe under a transverse magnetic field h_x . The superconducting transition temperature for p -wave order parameters T_{sc} is calculated and shows two domes as a function of h_x . We find strong enhancement of T_{sc} in the high-field dome near a saturation field h_s where the spins align in the transverse direction. Soft magnons generate strong attractive interactions there. Spin components of the pairing show a significant change between $h_x < h_s$ and $h_x > h_s$. We also discuss the appearance of superconductivity with zero-spin pair due to cancellation between external and exchange fields.

PACS numbers: 74.20.-z, 74.20.Mn, 74.25.-q

Ferromagnetic superconductivity (SC) has attracted much attention in condensed matter physics in the last decade.¹ U-based heavy-fermion compounds such as UGe₂, URhGe, UIr, and UCoGe show unconventional SC within their ferromagnetic phases.^{2–5} Non-unitary SC's⁶ are believed to appear in these compounds and both the SC and ferromagnetism are caused in the f electrons at U sites. Their pairing mechanism and symmetry as well as novel self-induced vortex states are central issues to be clarified in the modern theory of unconventional superconductors.

Two isomorphous compounds, UTe₂ (T =Rh, Co), exhibit SC at ambient pressure within their ferromagnetic state and have a similar Ising type anisotropy of magnetization.^{1,7} Spontaneous moment appears parallel to the c -axis and its magnetization curve exhibits meta-magnetism when magnetic field \mathbf{H} is applied to one of the hard axes (b axis) with a notable mass enhancement.⁸ This meta-magnetism is particularly prominent in URhGe and the moment gradually tilts with field and finally aligns parallel to \mathbf{H} at 12 T.⁹ Superconductivity appears below the transition temperature $T_{sc}=0.24$ K for $\mathbf{H}=\mathbf{0}$, and T_{sc} decreases with \mathbf{H} and disappears at 2 T for $\mathbf{H} \parallel b$.⁹ Interestingly, SC *reappears* above 8 T and shows the highest $T_{sc}=0.42$ K at 12 T.⁹

Theories of ferromagnetic SC have been developed by various groups,^{10–15} especially for UGe₂.^{16–19} In this paper, we focus on the reentrant SC in URhGe, which has not been investigated theoretically. The physics of the reentrant SC is quite different from that in UGe₂.^{16–18} The point is the presence of *soft* magnons in the Ising systems with transverse fields. We clarify it by extending the Scharnberg-Klemm (SK) theory²⁰ in the presence of ferromagnetism and transverse magnetic fields. In particular, we demonstrate (i) strong enhancement of T_{sc} near the saturation field, and (ii) strong field dependence in spin components (d -vector) of p -wave pairing.

We consider a system of conduction electrons as shown in Fig. 1, coupled to ferromagnetic localized spins, which have a magnetization \mathbf{M} in the z -direction (corresponding to the c axis in URhGe at $\mathbf{H}=\mathbf{0}$). We apply a transverse magnetic field H_x along the b axis and study its ef-

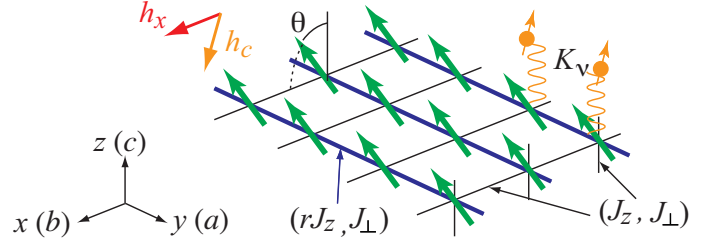


FIG. 1: (Color online) Schematic picture of the model.

fects on ferromagnetic SC. For conduction electrons, we use isotropic dispersion $\varepsilon_{\mathbf{p}}=\mathbf{p}^2/2m^*$, ignoring complex band structures.²¹ Here, \mathbf{p} and m^* are the momentum and the effective mass, respectively.

To model spin fluctuations in URhGe, we employ a simple model that can describe their essential behavior, and that is the ferromagnetic XXZ model.²² To discuss SC, we will later introduce couplings between localized spins and conduction electrons. We treat local and itinerant degrees of freedom separately and this is qualitatively justified in the “duality” picture.²³ There, ordered moments are due to the incoherent part of f electrons, while itinerant physics such as SC is described by quasiparticles with heavy effective mass m^* . In this paper, we denote magnetic moments and indices of the Kramers pairs simply as “spin,” but remember that these are complex combinations of orbital and spin moments in heavy-fermion systems.

The ferromagnetic XXZ model for localized moments is given as

$$H_S = - \sum_{\langle i,j \rangle} \left[J_{ij}^z S_i^z S_j^z + J_{\perp} \sum_{\nu=x,y} S_i^{\nu} S_j^{\nu} \right] - S h_x \sum_i S_i^x, \quad (1)$$

where the spins \mathbf{S}_i with $\mathbf{S}_i^2=S(S+1)$ are defined on a three-dimensional cubic lattice and $h_x \equiv \mu H_x / S$. $\mu=0.4\mu_B$ is the value of magnetic moment measured in experiment,³ where μ_B is the Bohr magneton. We have introduced spatial anisotropy J_{ij}^z as well as Ising spin anisotropy $J_{ij}^z > J_{\perp} > 0$ as shown in Fig. 1, since the crystal structure can be regarded as coupled-chains running in the $y(a)$ direction: $J_{ij}^z=J_z$ for bonds along \hat{x} or \hat{z} ,

while rJ_z along \hat{y} with $r > 0$. This spatial anisotropy lifts degeneracy in p -wave superconducting order parameters as will be discussed later. Although the tetragonal symmetry of the exchange couplings is higher than the orthorhombic one in URhGe, this is not essential for our discussions.

We analyze the model (1) for zero temperature $T=0$ by the linearized spin-wave approximation.²⁴ Due to the Ising anisotropy, the spontaneous moment points along \hat{z} at $h_x=0$. As h_x increases, the magnetization tilts toward \hat{x} with polar angle $\theta=\sin^{-1}(h_x/h_s)$ up to the saturation field $h_s=(4+2r)J_z-6J_\perp$. Magnons defined below describe transverse fluctuations around this tilted direction.

The magnon energy dispersion is expressed as $E_{\mathbf{q}}=S\sqrt{\epsilon_{\mathbf{q}}^2-4v_{\mathbf{q}}^2}$, where $\epsilon_{\mathbf{q}}=(c_\theta^2-s_\theta^2/2)h_s+h_x s_\theta-J_\perp(c_\theta^2+1)\gamma_{\mathbf{q}}-J_z s_\theta^2 \gamma_{\mathbf{q}}^y$, $2v_{\mathbf{q}}=s_\theta^2(h_s/2+J_z \gamma_{\mathbf{q}}^y-J_\perp \gamma_{\mathbf{q}})$ with $\gamma_{\mathbf{q}}=\sum_{l=x,y,z}(\cos ql-1)$, $\gamma_{\mathbf{q}}^y=\gamma_{\mathbf{q}}+(r-1)(\cos q_y-1)$, and $c_\theta(s_\theta)=\cos\theta(\sin\theta)$. The dispersion has an energy gap $S\sqrt{h_s^2-h_x^2}$ for $h_x < h_s$ and $S\sqrt{h_x(h_x-h_s)}$ for $h_x > h_s$. At $h_x=h_s$, the excitations are gapless $E_{\mathbf{q}\sim 0}\sim S\sqrt{h_s J_z(q_x^2+r q_y^2+q_z^2)}$. Note that the model (1) is ferromagnetic, and thus the linearized spin-wave approximation is fairly good even near h_s . Since the magnitude of S does not play an important role in our approximation, we set $S=1$. The renormalization of moment due to the quantum fluctuation is small and we neglect it hereafter.

Let us investigate the interactions of magnons and conduction electrons (quasiparticles). The quasiparticles feel the external field and exchange field via anisotropic antiferromagnetic Kondo coupling $K_{x,y,z}:\sum_{i\nu}K_\nu s_i^\nu S_i^\nu$ with s_i^ν being the spin of the quasiparticle at the site i . Again, note that this ‘‘spin’’ is, indeed, ‘‘pseudospin’’. Thus, in the mean field level, their energy dispersion is $\epsilon_{\mathbf{p}\pm}=\epsilon_{\mathbf{p}}\pm|\mathbf{h}_c|/2$ with $\mathbf{h}_c=(h_c^x, 0, h_c^z)\equiv(\mu_c H_x-K_x s_\theta, 0, -K_z c_\theta)$. Here, $\mu_c\equiv g^* \mu_B$ with the effective g -factor of quasiparticles g^* .

The lowest-order fluctuations beyond the mean-field approximation yield a magnon-quasiparticle interaction: $\sum_{i\nu}v_\nu a_i^\dagger \tilde{s}_i^\nu + \text{H.c.}$, where a_i^\dagger is a magnon creation operator at the site i and \tilde{s}_i^ν is the quasiparticle spin rotated such that the new z -axis is parallel to $-\mathbf{h}_c$. The coupling constant v_ν is given as $(v_x, v_y, v_z)=(K_z s_\theta \hat{h}_c^x + K_x c_\theta \hat{h}_c^z, -iK_y, K_z s_\theta \hat{h}_c^z - K_x c_\theta \hat{h}_c^x)/\sqrt{2}$ with $\hat{h}_c^{x,z}\equiv h_c^{x,z}/|\mathbf{h}_c|$.

Next, we derive linearized gap equations for p -wave SC²⁰ and determine the transition temperature T_{sc} and upper critical field H_{c2} . Since we are mainly interested in high-field states, we neglect small $4\pi\mathbf{M}$ less than ~ 1 kG in the magnetic induction.¹² This must be taken into account near $h_x=0$ and is important for discussions about self-induced vortex states, which is one of our future problems. Since $\mathbf{H}\parallel\hat{x}$, the gap equation for the p_x state $\vec{\Delta}_{xN}=[\Delta_{xN}^{++}, \Delta_{xN}^{--}, \Delta_{xN}^0]^T$ and the other orbitals $\{\vec{\Delta}_{yN}, \vec{\Delta}_{zN}\}$ are decoupled, where N represents the Landau level (LL), and ‘‘++’’, ‘‘--’’, and ‘‘0’’ denote the spin

projection of Cooper pairs along $-\mathbf{h}_c$. Different LL’s for the p_x state are decoupled to each other, while they are coupled for the (p_y, p_z) components. In the SK theory, the linearized gap equations are given as²⁰

$$\vec{\Delta}_{\alpha N} = \frac{3Tm^{*2}}{2\pi} \hat{V}_\alpha \sum_{N',\beta} \hat{S}_{NN'}^{\alpha\beta} \vec{\Delta}_{\beta N'}, \quad (\alpha, \beta \in \{x, y, z\}). \quad (2)$$

Here, \hat{V}_α is an interaction matrix of the spin part [see Eq.(3)] for the p_α state. \hat{S} includes both the Zeeman and orbital pair breaking effects and is diagonal in spin space.

\hat{V}_α is determined from the one-magnon exchange processes and we calculate this with the static approximation for the magnon Green’s function $D_{\mathbf{q}}(i\omega_m)=1/(i\omega_m-E_{\mathbf{q}})\sim-1/E_{\mathbf{q}}$. Averaging all the momentum dependence assuming p -wave gap functions $\eta_{\mathbf{p}}^\alpha$, \hat{V}_α is given as

$$\begin{aligned} \hat{V}_\alpha &= A_\alpha^+ v_z^2 \begin{pmatrix} 1 & w^2 & \sqrt{2}w \\ w^2 & 1 & -\sqrt{2}w \\ \sqrt{2}w & -\sqrt{2}w & w^2-1 \end{pmatrix} + A_\alpha^- v_y^2 \begin{pmatrix} 0 & 1 & 0 \\ 1 & 0 & 0 \\ 0 & 0 & -1 \end{pmatrix}, \\ &\equiv A_\alpha^+ v_z^2 \hat{V}_+(w) + A_\alpha^- v_y^2 \hat{V}_-, \end{aligned} \quad (3)$$

where $w=v_x/v_z$ and the first and the second columns of \hat{V}_α represent the equal spin pairing (ESP) with the spin function $|++\rangle$ and $|--\rangle$, respectively, while the third one represents the zero-spin pairing (ZSP) state $(|+-\rangle+|-+\rangle)/\sqrt{2}$. Note that ‘‘-’’ and ‘‘+’’ denote spins parallel and antiparallel to \mathbf{h}_c , respectively. Here,

$$A_\alpha^\pm \equiv \frac{1}{N_L^2} \sum_{\mathbf{p},\mathbf{k}} \eta_{\mathbf{p}}^\alpha \frac{e^{\pm 2\phi_{\mathbf{p}-\mathbf{k}}}}{E_{\mathbf{p}-\mathbf{k}}} \eta_{\mathbf{k}}^\alpha, \quad (4)$$

where the pairing form factor is chosen as $\eta_{\mathbf{p}}^\alpha = \sqrt{2} \sin p_\alpha$ and this corresponds to $\sqrt{3}p_\alpha$ in continuum systems.²⁰ $\phi_{\mathbf{p}-\mathbf{k}}$ is related to the Bogoliubov transformation: $\tanh 2\phi_{\mathbf{p}-\mathbf{k}} = 2v_{\mathbf{p}-\mathbf{k}}/\epsilon_{\mathbf{p}-\mathbf{k}}$, and N_L is the number of sites.

Before showing numerical results, we analyze \hat{V}_α for $h_x \sim h_s$. Since $E_{\mathbf{q}}$ is small around $\mathbf{q}=\mathbf{0}$, T_{sc} is expected to be enhanced. It is important to note that the direction of the local moments continuously changes toward $\pi/2$ for $h_x < h_s$, while $\theta=\pi/2$ above h_s . Expanded up to first order in $\delta\theta=\pi/2-\theta$, \hat{V}_α is given as

$$\frac{1}{2} \begin{pmatrix} 0 & A_\alpha^+ K_z^2 - A_\alpha^- K_y^2 & -\Gamma A_\alpha^+ \delta\theta \\ A_\alpha^+ K_z^2 - A_\alpha^- K_y^2 & 0 & \Gamma A_\alpha^+ \delta\theta \\ -\Gamma A_\alpha^+ \delta\theta & \Gamma A_\alpha^+ \delta\theta & A_\alpha^+ K_z^2 + A_\alpha^- K_y^2 \end{pmatrix}, \quad (5)$$

where $\Gamma = \sqrt{2}K_z^2\{[\mu_c h_s/(\mu_c K_z) - K_x/K_z]^{-1} - K_x/K_z\}$. For $h_x \geq h_s$, $\delta\theta=0$, and the gap equations for ESP and ZSP are decoupled. Note that the interaction is strongest for ZSP, since $A_\alpha^\pm > 0$. This is natural, since the spin fluctuations are transverse, which scatter quasiparticles with \pm spin into \mp spin states.

Low-field longitudinal fluctuations²⁵ also mediate interactions and we introduce a phenomenological ferromagnetic Ising interaction between quasiparticles:

– $\sum_{\langle i,j \rangle} J_{cc}^\alpha s_i^z s_j^z$, with $J_{cc}^\alpha > 0$ and $\alpha \in \{x, y, z\}$ is the direction of ij bond. As before, we include spatial anisotropy: $J_{cc}^{ij} = J_{cc}$ for bond $\parallel \hat{x}$ or \hat{z} , while $r'J_{cc}$ for bond $\parallel \hat{y}$. Then, the interaction kernel (3) is replaced as $\hat{V}_\alpha \rightarrow \hat{V}_\alpha + (\hat{h}_z^c)^2 J_{cc}^\alpha \hat{V}_+ (\hat{h}_x^c / \hat{h}_z^c) / 4$, with keeping the form (5) essentially unchanged.

Let us discuss the phase diagram of SC in the T - h_x space determined by our calculations. Figures 2 and 3 show the h_x -dependence of the SC transition temperature of the p_x - and $p_{y,z}$ -states for the isotropic ($r=r'=1$) and anisotropic ($r=1.2, r'=2$) cases, respectively. Figure 4 shows the spin part of the pairing, and will be discussed later. Our calculations show two domes of T_{sc} in the phase diagram, and this qualitatively reproduces the experimental data.⁹ One important observation is a strong enhancement and the presence of singularity in the high field dome at $h_x = h_s$. This manifests the change in the pairing state. The variations in the spin components are due to competition between the interaction strength and the Pauli depairing effects (PDE's) and we will examine this point in detail in the following.

Let us investigate how the PDE's influence pairing states. The PDE in the SK theory originates in the matrix \hat{S} in Eq.(2). For $h_x > h_s$, the ESP's and ZSP are decoupled as discussed above, which simplifies analysis. The PDE is weak when the exchange field nearly cancels the external field $h_c^x \sim 0$. This is realized at high field, and we expect there the ZSP state, since the corresponding interactions are strongest. This is the Jaccarino-Peter effect,²⁶ which was originally proposed for a rare earth ferromagnetic metal. When the cancellation is not sufficient and thus PDE is strong, the ZSP state is suppressed and the ESP state is favored. If the interactions are much stronger than the effective magnetic field, two ESP components $|++\rangle$ and $|--\rangle$, have nearly equal amplitude. If the interactions are not so strong, the ESP state with larger density of states (DOS) dominates

For $h_x \lesssim h_s$, the situation is more complex. When PDE is strong, the ESP with large DOS is realized as expected also for low field, while for weak PDE all the spin components contribute to the superconducting condensation, since the offdiagonal elements in \hat{V}_α are finite.

Now, we explain the details of Figs. 2–4. Our choice of parameters are: a mean-field ferromagnetic transition temperature $T_c^{\text{MF}} = J_z(2+r) = 10$ K, $H_s \equiv h_s / \mu = 10$ T, $m^*/m = 40$, $r'J_{cc} = 283$ K, $K_z = 109$ K, and $K_{x,y} = 0.3K_z$, where m is the bare electron mass. Electron density is set to 1 per unit cell and the lattice constant³ is set to 3.5 Å. Using these parameters, T_{sc} at $h_x = 0$ is $\simeq 0.6$ K for both parameter sets in Figs. 2 and 3.²⁷ g^* is the control parameter in our analysis below, which varies the Zeeman energy for quasiparticles.

Let us first examine the orbital part of pairing. The orbital motion couples only to the external field H_x as we mentioned above. Therefore, the p_x -pairing is always decoupled from the other orbitals and different LL's are decoupled there, while the p_y and p_z orbitals are mutually coupled with LL's also coupled. In the isotropic

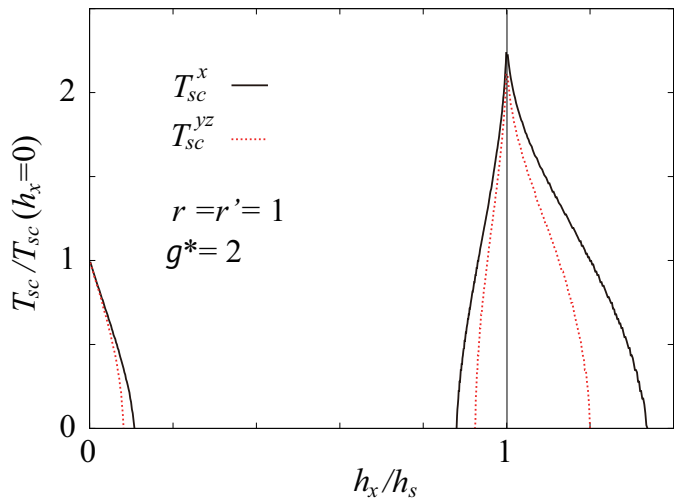


FIG. 2: (Color online) Dependence of transition temperature $T_{sc}^{x,yz}$ on transverse field h_x for $r=r'=1$ and $g^*=2$.

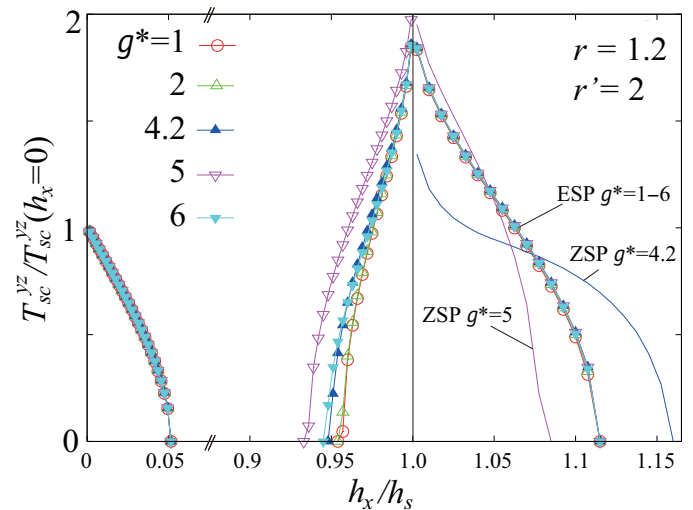


FIG. 3: (Color online) h_x -dependence of T_{sc}^{yz} for the anisotropic case $r=1.2, r'=2$ and five sets of g^* . The change of low-field dome with g^* 's is negligible. For $h_x > h_s$, the ZSP state is decoupled from the ESP state. Its T_{sc}^{yz} is shown by lines without symbols, except for $g^*=1, 2$, and 6, where T_{sc}^{yz} is nearly zero.

systems, the polar p_x -state with $N=0$ has the highest H_{c2} as shown in Fig. 2. We note that the $N=0$ LL plays a central role in both p_x and $p_{y,z}$ states.²⁰

When the interactions are spatially anisotropic in space with $r, r' \geq 1$, the p_x state is suppressed and a p_y -dominant state becomes stable, and *vice versa* for $r, r' \leq 1$. In the following, we analyze the former case, which is relevant for URhGe. Figure 3 shows T_{sc}^{yz} for $r=1.2$ and $r'=2$, as a typical case of strong anisotropies, for several values of g^* . Here, $T_{sc}^x \ll T_{sc}^{yz}$ for all the parameters and not shown. For the low-field SC, a p_y dominant state has a lower energy even for small $r' \gtrsim 1.05$, while less sensitive to r . This is because that the magnon gap is sufficiently large there and thus the transverse fluctuations are neg-

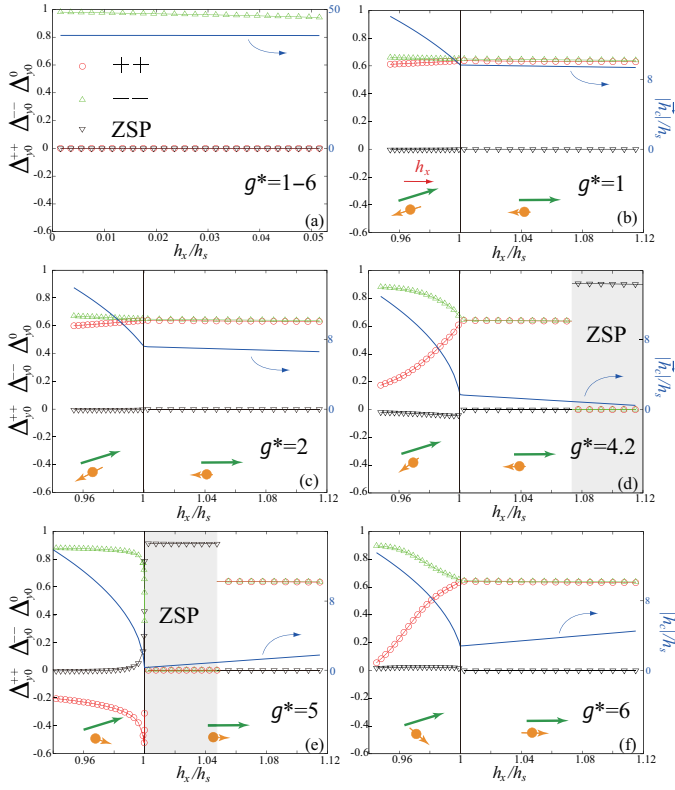


FIG. 4: (Color online) Spin part of p_y pairing in the $N=0$ LL for $r=1.2$ and $r'=2$: Δ_{y0}^{++} (\circ), Δ_{y0}^{--} (\triangle), and Δ_{y0}^0 (∇) at $T=T_{sc}^{yz}$. Lines represent $|\mathbf{h}_c|$. (a) Low-field part, g^* -dependence is negligible. (b)–(f) High-field part near h_s for various g^* 's. Localized moment (long arrow) and quasiparticle spin (short one with dot) are schematically shown. The magnitude of the quasiparticle spin is small ≤ 0.05 near h_s .

ligible. For the high-field SC, both r and r' affect its T_{sc} . Increasing r enhances T_{sc}^{yz} , while it suppresses T_{sc}^x . For the dependence on r' , increasing r' suppresses both T_{sc} 's. The suppression is stronger for T_{sc}^x than for T_{sc}^{yz} because the attractive force does not decrease for p_y pairs. It is also possible to realize a transition in the SC from p_x to $p_{y,z}$ symmetry or *vice versa*, as h_x increases, which is determined by the details of the anisotropies.

Second, we discuss the spin part of pairing, which is related to the d -vector of SC, and examine for the data in Fig. 3 the Zeeman effects with controlling g^* . Figure 4 shows the change in the spin part of pairing with h_x for the orbital component p_y and $N=0$ LL. They are calculated just at T_{sc}^{yz} and normalized as $\sum_N \sum_\alpha |\vec{\Delta}_{\alpha N}|^2 = 1$. Figure 4(a) shows the change in the low-field dome. We find that the g^* -dependence is negligible and the pairing is the ESP state with only one type of spin, which is parallel to the internal field \mathbf{h}_c , $|--\rangle$. This is consistent with the proposed gap symmetry for URhGe.²⁸ Figures 4(b)–4(f) show the results in the high-field dome. The region of $h_x > h_s$ is, in most of the cases, also the pure ESP state, but now the two spin components have almost the same amplitude. This is because $|++\rangle$ pairs are scat-

tered only to $|--\rangle$ pairs and *vice versa*, when $h_x > h_s$. However, their amplitude difference may become larger depending on g^* and $|\mathbf{h}_c|$. In the region of $h_x < h_s$, a small amplitude of the ZSP component hybridizes. The two ESP components are still dominant, but their difference is now larger and the h_x -dependence is noticeable, particularly for larger g^* 's. For all g^* 's, transverse spin fluctuations near h_s favor the linear combinations of two ESP states, while ZSP is suppressed by the PDE, except for some regions in Figs. 4(d) and 4(e) as we discuss below.

The quasiparticle spins respond to both the exchange field of the localized moments and the external magnetic field, and g^* controls the latter part. Thus, varying g^* affects the angle between the quasiparticle and the localized spins as schematically depicted in Figs. 4(b)–4(f). When the external and exchange fields are canceled, $\mathbf{h}_c = \mathbf{0}$, the quasiparticle spins feel no field. Indeed, the cancellation can become nearly perfect for $g^* = 4.2$ and 5. This leads to emergence of ZSP states (Jaccarino-Peter effect),²⁶ and occurs in the shaded regions in Figs. 4(d) and 4(e). When h_s is close to the point $|\mathbf{h}_c| \sim 0$ as in Fig. 4(e), the expansion in Eq.(5) is not sufficient, and this results in the almost vertical slope of $\vec{\Delta}_{y0}$ for $h_x \lesssim h_s$, but this situation is not of main interest in this paper.

Let us finally comment about URhGe. We have succeeded in reproducing the overall phase diagram and two SC domes as shown in Figs. 2 and 3. The transition temperature for the second dome shows strong enhancement near h_s . The superconducting gap symmetry is basically equal-spin $p_{y(a)}$ -pairing for both domes. It is $|--\rangle$ for the low-field, and $\sim (|++\rangle + |--\rangle)/\sqrt{2}$ for the high-field SC. The gap functions have a point node due to the finite ip_z component, but since its amplitude is very small, it might be difficult to experimentally distinguish this from that with a line node. Detecting the change in the spin components of pairing near h_s is an experimental test for the present theory. Exploring the sudden change in pairing symmetry due to the Jaccarino-Peter effect is another interesting challenge in this field.

For a more precise theoretical analysis, one should take into account the optimization of form factor $\eta_{\mathbf{k}}^\alpha$, longitudinal spin fluctuations for $h_x \lesssim h_s$,⁹ the weak first-order transition,⁹ the variations of the Fermi surfaces near h_s ,²⁹ and anisotropy in the effective mass,¹⁵ which might improve quantitative agreement between our theory and experiments. Our main conclusion for the superconducting order parameters for $h_x \sim h_s$ is that the pairing interaction prefers mixing $|++\rangle$ and $|--\rangle$ and this is in clear contrast to nearly pure $|--\rangle$ state, which is selected by Zeeman energy. Difference in their amplitudes depends on the details, and a more quantitative analysis about this is one of our future plans.

K. H. thanks Dai Aoki for fruitful discussions. He is supported by KAKENHI (No. 30456199) and by a Grant-in-Aid for Scientific Research on Innovative Areas ‘‘Heavy Electrons’’ (No. 23102707) of MEXT, Japan.

-
- ¹ See, recent review: D. Aoki and J. Flouquet: J. Phys. Soc. Jpn. **81**, 011003 (2012).
- ² S. S. Saxena, P. Agarwal, K. Ahilan, F. M. Grosche, R. K. W. Haselwimmer, M. J. Steiner, E. Pugh, I. R. Walker, S. R. Julian, P. Monthoux, G. G. Lonzarich, A. Huxley, I. Sheikin, D. Braithwaite, and J. Flouquet, Nature **406**, 587 (2000).
- ³ D. Aoki, A. Huxley, E. Ressouche, D. Braithwaite, J. Flouquet, J.-P. Brison, E. Lhotel, and C. Paulsen, Nature **413**, 613 (2001).
- ⁴ T. Akazawa, H. Hidaka, H. Kotegawa, T. C. Kobayashi, T. Fujiwara, E. Yamamoto, Y. Haga, R. Settai, and Y. Ōnuki J. Phys. Soc. Jpn. **73**, 3129 (2004).
- ⁵ N. T. Huy, A. Gasparini, D. E. de Nijs, Y. Huang, J. C. P. Klaasse, T. Gortenmulder, A. de Visser, A. Hamann, T. Görlach, and H. v. Löhneysen, Phys. Rev. Lett. **99**, 067006 (2007).
- ⁶ T. Ohmi and K. Machida, Phys. Rev. Lett. **71**, 625 (1993).
- ⁷ W. Knafo, T. D. Matsuda, D. Aoki, F. Hardy, G. W. Scheerer, G. Ballon, M. Nardone, A. Zitouni, C. Meingast, and J. Flouquet, Phys. Rev. B **86**, 184416 (2012).
- ⁸ A. Miyake, D. Aoki, and J. Flouquet, J. Phys. Soc. Jpn. **77**, 094709 (2008).
- ⁹ F. Lévy, I. Sheikin, and A. Huxley, Nat. Phys. **3**, 460 (2007), F. Lévy, I. Sheikin, B. Grenier, C. Marcenat, and A. Huxley, J. Phys. Condens. Matter **21**, 164211 (2009).
- ¹⁰ D. Fay and J. Appel, Phys. Rev. B **22**, 3173 (1980).
- ¹¹ T. R. Kirkpatrick and D. Belitz, Phys. Rev. B **67**, 024515 (2003).
- ¹² V. P. Mineev, Phys. Rev. B **66**, 134504 (2002), K. V. Samokhin and M. B. Walker, Phys. Rev. B **66**, 174501 (2002).
- ¹³ V. P. Mineev, Phys. Rev. B **81**, 180504(R) (2010), *ibid.*, **83**, 064515 (2011).
- ¹⁴ Y. Tada, N. Kawakami, and S. Fujimoto, J. Phys. Soc. Jpn. **80**, SA006 (2011).
- ¹⁵ C. Lösscher, R. A. Klemm, J. Zhang, and Q. Gu, arXiv:1110.6667, C. Lösscher, J. Zhang, Q. Gu, and R. A. Klemm, arXiv:1210.7442.
- ¹⁶ K. G. Sandeman, G. G. Lonzarich, and A. J. Schofield, Phys. Rev. Lett. **90**, 167005 (2003).
- ¹⁷ A. H. Nevidomskyy, Phys. Rev. Lett. **94**, 097003 (2005).
- ¹⁸ J. Linder, I. B. Sperstad, A. H. Nevidomskyy, M. Cuoco, and A. Sudbø, Phys. Rev. B **77**, 184511 (2008).
- ¹⁹ D. V. Shopova and D. I. Uzunov, Phys. Rev. B **79**, 064501 (2009).
- ²⁰ K. Scharnberg and R. A. Klemm, Phys. Rev. B **22**, 5233 (1980).
- ²¹ M. Diviš, L. M. Sandratskii, M. Richter, P. Mohn, P. Novák, J. Alloys Compd. **337**, 48 (2002), A. B. Shick, Phys. Rev. B **65**, 180509(R) (2002).
- ²² Essentially the same results are obtained in presence of single-ion anisotropy.
- ²³ Y. Kuramoto and K. Miyake, J. Phys. Soc. Jpn, **59**, 2831 (1990).
- ²⁴ T. Holstein and H. Primakoff, Phys. Rev. **58**, 1098 (1940).
- ²⁵ T. Hattori, Y. Ihara, Y. Nakai, K. Ishida, Y. Tada, S. Fujimoto, N. Kawakami, E. Osaki, K. Deguchi, N. K. Sato, and I. Satoh, Phys. Rev. Lett. **108**, 066403 (2012).
- ²⁶ V. Jaccarino and M. Peter, Phys. Rev. Lett. **9**, 290 (1962).
- ²⁷ We have introduced a cutoff $\Lambda = \exp[\langle \ln \omega \rangle]$, where $\langle \cdot \rangle$ denotes spectral average measured by $-\pi^{-1} \text{Im} D_{\mathbf{q}}(\omega + i0)/\omega$; P. B. Allen and R. C. Dynes, Phys. Rev. B **12**, 1027 (1975).
- ²⁸ F. Hardy and A. D. Huxley, Phys. Rev. Lett. **94**, 247006 (2005).
- ²⁹ E. A. Yelland, J. M. Barraclough, W. Wang, K. V. Kamenev, and A. D. Huxley, Nat. Phys. **7**, 890 (2011).